Then taking the first derivative with respect to pressure, we have

$$\left(\frac{\partial K_s}{\partial p}\right)_s = \left(\frac{\partial \rho}{\partial p}\right)_s (a + b\rho)^2 + 2b\rho\,(a + b\rho)\left(\frac{\partial \rho}{\partial p}\right)_s .$$

Since the bulk modulus is given by $K_s \equiv \rho\,(\partial p/\partial \rho)_s$, we can obtain from eqs. (2) and (3) that

$$\left(\frac{\partial K_s}{\partial p}\right)_s = 1 + \frac{2b\rho}{V_\phi} = 1 + 2b\rho\,(\rho/K_s)^{\frac{1}{2}} \qquad (4)$$

By using $b = 2.65$ (km/sec)/(g/cm^3) *, the author tested in table 1 the compatibility of eq. (4) with experimental $(\partial K_s/\partial p)_T$ values for all those oxides and silicates about the mean atomic weight of 20 to 21, which have been determined in recent years by ultrasonic methods. In all cases, the calculated $(\partial K_s/\partial p)_s$ values are smaller than the experimental $(\partial K_s/\partial p)_T$ values determined on the same material; the calculated values, relative to the measured $(\partial K_s/\partial p)_T$, were about 27% smaller for quartz, about 26% smaller for olivine, about 15% smaller for spinel, about 13% smaller for periclase and about 12% smaller for corundum. The greater the bulk modulus of material, the smaller the difference between the measured and calculated values of $(\partial K_s/\partial p)$. Thus, a correction term (C/K_s) to eq. (4) is necessary; it arises from our observation that the difference between the measured and calculated values of $(\partial K_s/\partial p)$ is inversely proportional to the bulk modulus of material. Rewriting eq. (4) with this correction term, we have then

$$\left(\frac{\partial K_s}{\partial p}\right)_s \simeq 1 + \frac{2b\rho}{V_\phi} + \frac{C}{K_s}, \qquad (5)$$

where, to the first-order approximation, C is one in the same units of K_s (in Mb). Thus, the effect of the correction term (C/K_s) on $(\partial K_s/\partial p)_s$ is large for materials of small K_s, but for materials of large K_s the correction becomes relatively small. Using eq. (5), $(\partial K_s/\partial p)_s$ for quartz, olivine, periclase, spinel and corundum are newly calculated; the calculated $(\partial K_s/\partial p)_s$ values for these materials are, respectively, 7.3, 4.6, 4.4, 4.1 and 4.1 and these values compare favorably with experimental $(\partial K_s/\partial p)_T$ values of 6.5 (±0.3), 5.0 (±0.3), 4.3 (±0.2), 4.3 (±0.3), and 4.2 (±0.2) as reported in the literature [5, 6]. It is then seen that eq. (5) could be used for estimating the value of $(\partial K_s/\partial p)_s$ for crystalline solids for which ultrasonic-pressure experiments are limited by the present state of technology involving material synthesis and characterization.

The usefulness of eq. (5), and also the thought behind it, is apparent since the quantities like b, V_ϕ, ρ and K_s can be obtained readily as outlined in earlier paragraphs. Rigorously speaking, the parameter $(\partial K/\partial p)$ enters into equations describing the pressure-volume relationships in solids. The difference arising from thermodynamic corrections as detailed elsewhere [7] between the $(\partial K_s/\partial p)_s$ value resulting from eq. (5) and $(\partial K/\partial p)_T$ or that between the experimental $(\partial K_s/\partial p)_T$ and the calculated $(\partial K_s/\partial p)_s$ is about 1–2% each. For all practical purposes in geophysics, these corrections can be ignored and we use the $(\partial K_s/\partial p)_s$ values in the following discussion.

3. Illustration of the scheme

Some examples for illustrating the use of eqs. (3) and (5) follow. The first example is concerned with finding the equations of state for the spinel phase formed under pressure from the olivine structure in the $(Mg, Fe)_2 SiO_4$ system. In table 2 (part A), the density ρ and the bulk sound velocity V_ϕ of olivine-transformed spinels are tabulated. From these ρ and V_ϕ values, K_s and $(\partial K_s/\partial p)_s$ are calculated according to eqs. (3) and (5), respectively; the results are entered in the table for three $(Mg_x Fe_{1-x})_2 SiO_4$-spinels. Using these EOS parameters, the volume-pressure trajectories inferred from the Birch equation of state [1] are shown in fig. 1 for olivines and the olivine-transformed spinels. Superimposed on this figure are the data points resulting from isothermal compression experiments by Mao et al. [8] for three iron-rich spinels transformed under pressure from their respective olivine structures. It is clearly seen in fig. 1 that, although the present comparison is made for a pressure range of about 15% of the bulk modulus, there is strong

* Based on the ultrasonic velocity data in table 1, the V_ϕ values of 35 data points for 22 substances (whose mean atomic weights range from 20 to 21) are fitted to eq. (2) by a least squares method. The coefficients in eq. (2) are found to be $a = -2.59$ (km/sec) and $b = 2.65$ (km/sec)/(g/cm^3); the correlation coefficient is 0.96 and the standard error is 0.14 (km/sec). This value of b is in good agreement with $b = 2.59$ (km/sec)/(g/cm^3) found earlier by Wang [4].

Table 2
Equation of state parameters of olivine-transformed spinels, coesite and stishovite of silica polymorphs and the possible high-pressure phases of pyroxene.

High-pressure phase	Density (g/cm^3)	V_ϕ (km/sec)	K_s (Mb)	$\frac{\partial K_s}{\partial p}$
Part A:				
β-Mg_2SiO_4	3.556	7.24	1.86	4.1
γ-$(Mg, Fe)_2SiO_4$	3.800	6.78	1.93	4.8
γ-Fe_2SiO_4	4.849	6.35	1.96	5.5
Part B:				
Coesite	2.920	4.70	0.65	5.8
Stishovite	4.287	9.8	4.1	3.4
Part C:				
(1) Garnet	3.64	6.55	1.56	4.6
(2) Spinel + stishovite	3.77	6.82	1.75	4.5
(3) Ilmenite	3.85	7.08	1.91	4.3
(4) Oxides-mixture	4.08	7.50	2.32	4.2
(5) Perovskite	4.35	8.10	2.83	4.1
Estimated uncertainty %	0.5	5	5	10

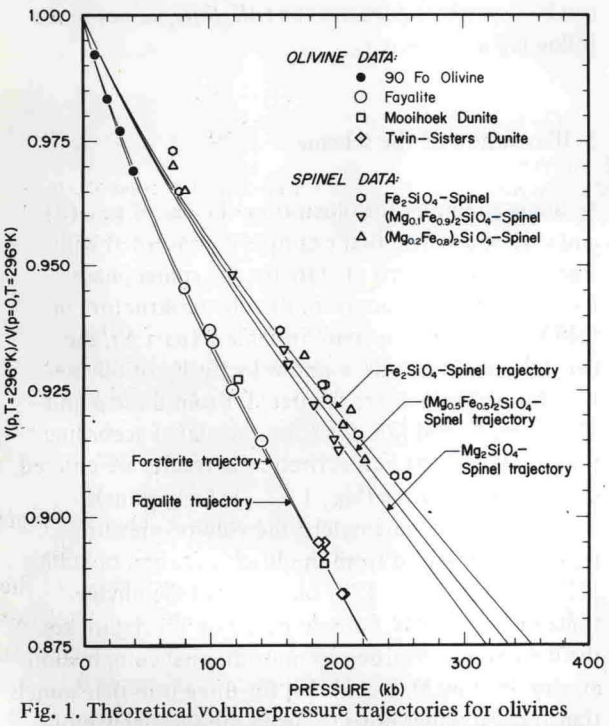

Fig. 1. Theoretical volume-pressure trajectories for olivines and olivine-transformed spinels; comparison with isothermal compression data. The solid lines are the results of the present theory, and they are independent of the compression data points.

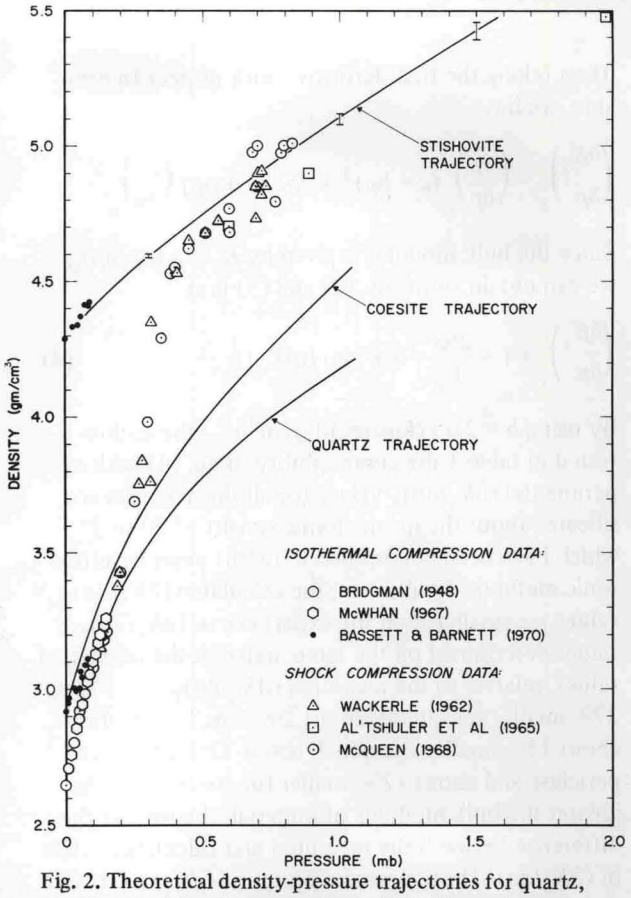

Fig. 2. Theoretical density-pressure trajectories for quartz, coesite and stishovite; comparison with isothermal compression data and shock-wave data points. The solid lines are the results of the present theory and they are independent of the compression data points.

evidence of agreement between the theoretical volume-pressure trajectories and the experimental compression data for the olivine-transformed spinels.

The second example deals with the equations of state of silica polymorphs under pressure. Quartz, stable at ambient conditions, transforms to coesite at about 20 kb pressure and then to stishovite at pressures above 90 kb. With the use of the scheme proposed here, the author finds the EOS parameters of coesite and stishovite as tabulated in table 2 (part B). As in the first example with spinels, the density-pressure trajectories resulting from the Birch equation of state with the parameters listed in table 2 (Part B) are shown in fig. 2. Superimposed on this figure with these trajectories are isothermal compression data points of Bridgman [9], McWhan [10], and Bassett and Barnett [11] for quartz, coesite and stishovite phases, respectively. Also superimposed on the present density-pres-